Optics Communications 392 (2017) 25–30

Contents lists available at ScienceDirect

Optics Communications

journal homepage: www.elsevier.com/locate/optcom

Photon-limited depth and reflectivity imaging with sparsity regularization

Kang Yan[a,b], Li Lifei[a], Duan Xuejie[c], Zhang Tongyi[a,*], Li Dongjian[a], Zhao Wei[a]

[a] State Key Laboratory of Transient Optics and Photonics, Xi'an Institute of Optics and Precision Mechanics, Chinese Academy of Sciences, Xi'an 710119, China
[b] University of Chinese Academy of Sciences, Beijing 100049, China
[c] School of Physics and Optoelectronic Engineering, Xidian University, Xi'an 710071, China

ARTICLE INFO

Keywords:
Photon-limited imaging
3D imaging lidar
Sparsity regularization
Total variation

ABSTRACT

We demonstrate a depth and reflectivity imaging system at low light level based on sparsity regularization method. Depth and reflectivity imaging from the time-correlated single photon counting (TCSPC) measurement in limit of few photon counts are reconstructed through exploiting transform-domain sparsity. Two different sparsity-based penalty function: total variation (TV) penalty and l_1 norm penalty measuring sparsity in the discrete cosine transform(DCT) basis, are applied to the experimental data. The results show that compared with traditional image denoising method, sparsity regularization approach achieves better accuracy with fewer photon measurements. Further more, the performance of TV regularization is proved better than l_1-DCT regularization method for photon-limited imaging at first time, especially in the case of depth imaging. Our system is a photon-limited imaging device for a variety of applications, such as target detection, space surveillance, and distance measurement.

1. Introduction

Photon-limited imaging has attracted huge attention for a range of applications (e.g., target detection, space surveillance, and distance measurement) due to its unique ultralow-light working mode [1–5]. There are two key components in this imaging system. One is the detector with single photon sensitivity. While the Geiger-mode single photon detector (GmAPD) is already well developed and commercially available [6–9]. Another one is time-correlated single photon counting (TCSPC) module. TCSPC is a statistical sampling technique with picoseconds timing resolution based on the repetitive, precisely timed registration of single photons [10–14]. Previous research about the depth and reflectivity imaging based on GmAPD introduced many different methods to improve the efficiency of the imaging system at low light level. MIT Lincoln Laboratory used a GaSb-based material system 32×32 GmAPD array to extend to 2 μm wavelength operation, achieving 30 cm depth resolution at a distance of 20 m [15]. McCarthy et al. [16] used a low noise superconducting nanowire single-photon detector in their 1560 nm wavelength laser ranging system which obtained centimeter resolution depth images in daylight at stand-off distances of the order of one kilometer. A composite modulation method was used based on GmAPD in Ref. [17] to achieve the range-intensity image of a target in low-light level environments. The above and some other traditional imaging lidar systems which use single photon detector and TCSPC technique usually needs to detect hundreds of photons per pixel and even more data needs to be collected in the presence of background noise [18]. The resulting long dwell times limit the real-time performance of imaging lidar systems and lower the achievable imaging quality by fast raster scanning. Meanwhile, it is typical to first obtain a noisy pixelwise maximum likelihood (ML) estimate of scene reflectivity and depth using photon arrival data then applying image denoising methods. However, under low light level conditions the sample data is limit and signal-to-noise ratio (SNR) is low, ML solutions get inaccurate estimates. In addition, the traditional denoising methods usually assume a Gaussian noise model [19], which is appropriate for high-flux situations but not for low light levels. Therefore, it is necessary to develop a novel imaging system under the condition of low light level and low SNR.

When the number of the photons is small, the measurement process is best modeled with a Poisson distribution [19,20]. Thus, accurate reconstruction of a spatial or temporal image from Poisson data can be accomplished by minimizing a negative Poisson log-likelihood objective function with non-negativity constraints [19]. Actually, natural scenes possess a typical scene structure–in depth as well as in reflectance–which is often described using sparsity in appropriate transform domains, such as discrete wavelet transform (DWT) or

* Corresponding author.
E-mail addresses: kangyan@opt.ac.cn (K. Yan), lilifei@opt.ac.cn (L. Lifei), duan1130@126.com (D. Xuejie), tyzhang@opt.ac.cn (Z. Tongyi), lidongjian@opt.ac.cn (L. Dongjian), weiz@opt.ac.cn (Z. Wei).

http://dx.doi.org/10.1016/j.optcom.2017.01.032
Received 28 November 2016; Received in revised form 20 January 2017; Accepted 21 January 2017
Available online 28 January 2017

discrete cosine transform (DCT). Therefore, a regularization term is always added to constrain the sparsity of the underlying image over the transform domain. In Ref. [4,21], the l_1 norm based on DWT is applied to constrain the sparsity of image. In Ref. [22,23], total variation (TV) seminorm is selected as the regularization term. TV seminorm is essentially l_1 norm of derivative [24]. Instead of assuming the signal is sparse, the premise of TV regularization is that the gradient of the underlying signal or image is sparse. In general, this seminorm measures how much an image varies across pixels [25], which is often a useful alternative to DWT or DCT based regularizer. Although TV regularization can be regarded as a generalized l_1 regularization, for comparative purpose we distinguish it from l_1 regularization here.

In this paper, we demonstrate a photon-limited depth and reflectivity imaging system by using sparsity regularization from a small number of photon measurements at each pixel, even the mean count of the flux reaching the detector approaches 1.8 photons per pixel. When the scanning single photon detector is replaced with a single photon detector array with time-correlated or time-resolved function [26], this scanning imaging setting will form a genuine photonic camera, which can reconstruct 3D images of scenes only with a few photons per pixel. Compared with the conventional two-step procedure of pointwise ML estimation followed by traditional denoising method, the sparsity regularization methods achieve better image quality with fewer photon measurements. The experimental results show that performance of TV regularization is proved better than l_1-norm regularization for photon-limited imaging at first time, especially in the case of depth imaging.

2. Experiments

The imaging system schematically illustrated in Fig. 1 is used to collect the photon arrival data. The illumination source is a supercontinuum laser (SuperK EXTREME EXW-12, NKT Photonics, Denmark) with tunable wavelength and tunable repetition rate. In this experiment, the wavelength was selected as 532 nm by an acousto-optic tunable filter and the repetition rate was set at 3.89 MHz. The average power was set at 10 μW. The laser beam was collimated by lenses L1 and L2. A half-wave plate (HWP) was located before the polarization beam splitter (PBS) to control the transmission of the laser pulse at PBS. The laser output was reflected off a Thorlabs GVS012 two-axis galvo scanning system that raster scanned the beam over the target. The maximum mechanical scan angle was $\pm 20°$, which limits the field of view (FOV) of imaging system. The galvo system took two analog voltage inputs (one for each axis, 0.5 V/degree) supplied by a Tektronix AFG 3252 function generator that was programmed by LabVIEW. The target was placed at distance of 1.5 m apart from the experimental set up. The diameter of the spot size at 1.5 m distance was measured to be 2 mm. The scattered light in the FOV of the system returned to the GmAPD through PBS reflection. Before detection, the light was filtered using an optical band pass filter (BPF) with 1 nm bandwidth centered at 532 nm whose peak transmission was 20%. The GmAPD was a Perkin Elmer series detector (SPCM-AQRH-16) with 180 μm active area, 55% quantum efficiency at 532 nm, less than 100 ps time jitter, and less than 25 dark counts per second. The photon detection events were time stamped relative to the laser pulse with 8 ps

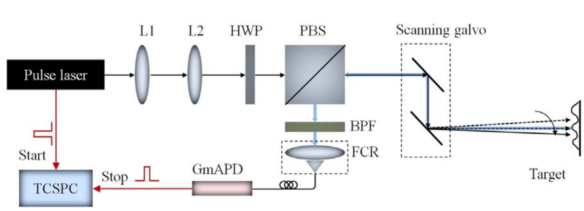

Fig. 1. Schematic of imaging system which comprises a supercontinuum laser source, a GmAPD detector, a TCSPC module and a custom transceiver. Optical components include: collimation lenses (L1, L2); half wave plate (HWP); polarizing beam splitter (PBS); scanning galvo mirrors; optic bandpass filter (BPF); fiber coupling receiver (FCR).

resolution using HydraHarp400 TCSPC module (PicoQuant). The characteristic of the complete TCSPC system that summarizes its overall timing precision is its Instrument Response Function (IRF) [14]. The IRF was obtained by directly scattering the detector with highly attenuated laser and binning the photon arrival times to genereate a histogram of photon counts. The IRF width of our imaging system was measured as 448 ps.

We had tried two different transmit-receive modes, bistatic and monostatic, during the experiments. These two modes have their own advantages and disadvantages. The advantages of the bistatic include simple optical setup and no internal reflection interference. However, because of the fixed receiver optical system and the larger FOV for receiving, more background light comes to the receiving system. As to the monostatic system, the influence of back light is much less than that of bistatic, because only the back light from the illuminated area on the target can project into the detector. However, its disadvantages include more difficult adjustment of the optical path and effective isolation between the transmitting and receiving beams (e.g., internal reflection). Finally, the monostatic system is adopt as Fig. 1 showing and the internal reflection was removed during data processing. For the data acquisition part, a HydraHarp400 time-tagged time resolved (T3) measurement mode was adapted. The resulting HT3 files are read using a mixed programming of MATLAB and Perl. This program discarded the useless information such as parameter setting log and overflow marker except for the photon detection events.

To generate one complete data set, we raster scanned over 200×200 pixels with two-axis galvo system. Each pixel was illuminated with a total of N light pulses. The pixel-wise data acquisition time is then $T_a = T_r \times N$ seconds. Here T_r is determined by the repetition rate. We record the total number of observed photon detections $k_{i,j}$ along with their set of photon arrival times $T_{i,j} = \{t_{i,j}^{(1)}, t_{i,j}^{(2)}, \ldots, t_{i,j}^{(k_{i,j})}\}$ at each pixel. If $k_{i,j} = 0$, then $T_{i,j} = \varnothing$. The measurement uncertainty in the photon arrival time results from background light intensity b and dark counts d. Before collecting the data, we measured the dark counts of the system as ~20 counts/s when turning off all light in the lab. The sum value of the background light and dark counts is measured as ~382 counts/s when turning on one lab lamp. The laser power was adjusted so that each photon detection had about 50% probability of originating from background light, i.e, the SNR is equal to 1. Namely, SNR is defined as the mean detections due to backreflected light divided by the mean detections due to background light and dark counts.

3. Data processing procedure

In this section, we demonstrate the 3-step computational reconstruction procedure using to recover high quality scene reflectivity and depth imaging from few photon arrival data. This framework was first developed in [4], and modified in [23,27], which proceeds in three steps. To our knowledge, the penalty term is also important in the framework, which can affect the results of reconstruction. Therefore, we used and compared two different penalty functions: total variation penalty and l1 norm penalty, the detail information is described later in this section and Section 4.

Illuminating a scene pixel (i,j) with intensity-modulated light pulse $s(t)$ results in backreflected light signal $r_{i,j}(t) = x_{i,j} s(t - 2z_{i,j}/c) + b$, where x denotes target reflectivity, z denotes the distance to target patch and c denotes the speed of light. The indices $i = 1, \ldots, xp$ and $j = 1, \ldots, yp$ represent the horizontal and vertical pixel coordinates, respectively. The quantum nature of light is correctly accounted for taking the counting process at the GmAPD output to be an inhomogeneous Poission process with rate funtion: $\lambda_{i,j}(t) = \eta r_{i,j}(t) + d = \eta x_{i,j} s(t - 2z_{i,j}/c) + (\eta b + d)$, where η denotes the detection efficiency. For notational convenience, the mean signal S and background count B per period are defined as $S = \int_0^{T_r} s(t)dt$ and